

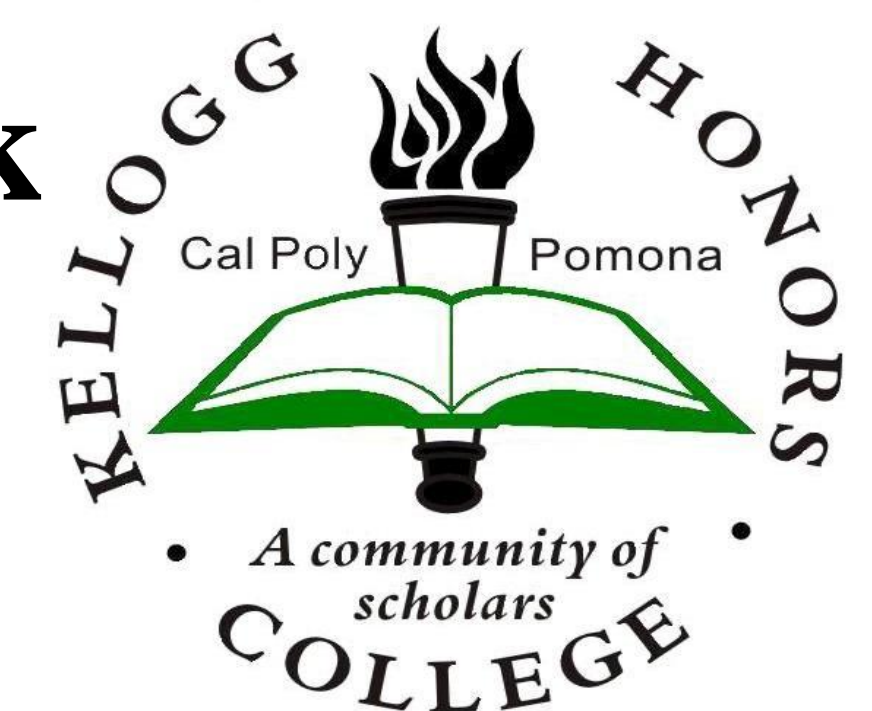
Graphene-Based Coating on Stainless Steels for Proton Exchange Membrane Fuel Cells



Brooke Singleton, Shehab Bassiouni, Fiona Follett, Sean Vinik
Chemical and Materials Engineering

Mentor: Dr. Vilupanur Ravi

Kellogg Honors College Capstone Project



Introduction:

Replacing fossil-fuel burning vehicles with zero emission electrochemically powered vehicles has the potential to mitigate fossil fuel usage. The proton exchange membrane fuel cell (PEMFC) is a viable solution due to its low operating temperatures, high efficiency, and zero emission. In order for PEMFCs to be commercially available in a competitive market, a cost-effective material needs to be selected. Current target goals set by the Department of Energy (DOE) for bipolar plates require the selected materials to be durable, have a high corrosion resistance, high electrical conductivity, and low density.

Background:

Currently, the endplates of fuel cell stacks for stationary applications are made from graphite. Though graphite offers excellent corrosion resistance, its porous nature makes it difficult to shape into thin sheets and its brittleness makes it unsuitable for transportation applications. In addition, the cost of manufacturing graphite causes the separator plates to account for 60% of the fuel cell cost.¹ Metallic bipolar plates exhibit desirable mechanical and electrical properties for bipolar plate applications in PEMFCs. Additionally, these materials offer a cost-effective replacement for graphite. However, candidates for metallic bipolar plates may be susceptible to corrosion. In addition, corrosion-resistant materials, e.g., stainless steel, can form a passive surface layer that can significantly increase its contact resistance.²

To meet the twin requirements of corrosion resistance and electrical conductivity, one approach would be to modify the surface of candidate alloys such as stainless steels. Recently, graphene has emerged as a promising candidate for surface modification of metallic materials.

Due to its low density, high electrical conductivity, and resistance to corrosion, graphene offers an ideal coating for stainless steel plates to be used.³

Objective:

Characterization and comparison of corrosion resistance for uncoated and surface modified UNS S41000 in a PEMFC environment at 70°C.

Methods and Materials:

Graphene oxide was prepared using the Tour Method.⁴ A powder mixture of graphite and KMnO_4 were dissolved in an acid solution containing H_2SO_4 and H_3PO_4 . Isothermal conditions were maintained using an ice and water mixture. The acid solution was subsequently placed on a hot plate and stirred for 12 hours at 50°C. After cooling to room temperature, the solution was poured into a beaker containing frozen deionized water, followed by 3 mL H_2O_2 . Sufficient time was allowed for precipitation of graphene oxide (GO) followed by settling. Washing and decanting was performed with tap water until the solution attained neutrality. The supernatant was poured off and the remaining solid was dried in a furnace at 45°C. The isolated graphene oxide was washed multiple times with 10 wt% HCl and DI water with a vacuum filter. The solid was then dried in a furnace at 45°C. The produced GO was characterized by X-Ray diffraction and scanning electron microscopy.

A copper layer was electroplated onto UNS S41000 at 1.5V for 15 minutes. The copper-plated coupon was placed in a bath containing 4 wt% GO solution at 8V for 10 minutes. The plated coupon was then dried in the furnace at 45°C.

The uncoated metal coupons were ground in succession from 240 to 600 SiC grit paper. The uncoated and coated coupons were electrochemically characterized using 0.01M HCl and 0.01M Na_2SO_4 solution at 70°C per ASTM G59 protocols. Open circuit potential (OCV) measurements were first conducted for 1 hour, followed by a linear polarization resistance (LPR) scan in the ± 25 mV range and finally a potentiodynamic scan in the ± 400 mV range. Additional reduction methods were also explored, by annealing the graphene oxide coated coupons in an inert atmosphere at 500°C for 2 hours.

References:

1. B. Cunningham, et al. Journal of Materials Chemistry. 16 (2006) 4385
2. T. Chiang, et al. International Journal of ELECTROCHEMICAL SCIENCE. 10 (2015) 9556.
3. W. Spoutter, et al. Journal of Nanomaterials. 13 (2013) 116
4. D. Marcano, et al. ACS Nano. 4 (2010) 4806
5. L. Stobinski, et al. Journal of Electron Spectroscopy and Related Phenomena. 195 (2014) 145.
6. Y. Choi, et al. Molecules. 21 (2016) 375
7. S. Drewniak, et al. Polish Journal of Chemical Technology. 17 (2015) 109

Results:

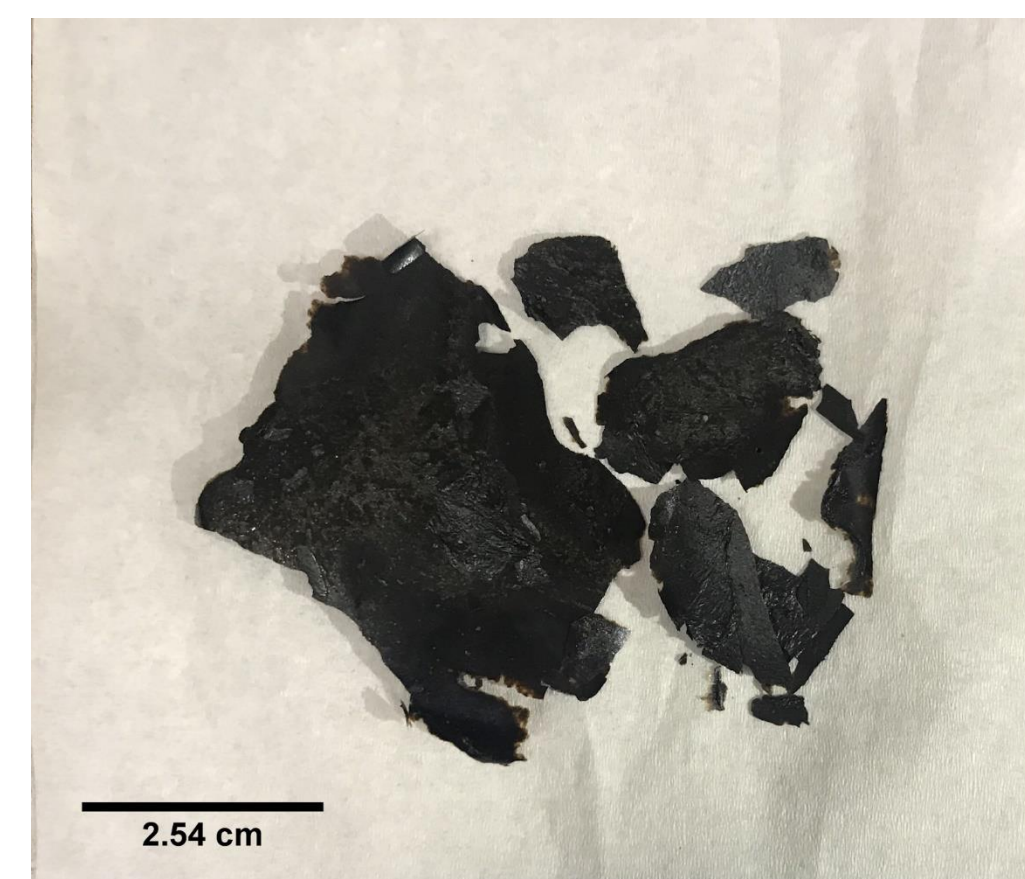


Figure 1: Macro image of dried graphene oxide

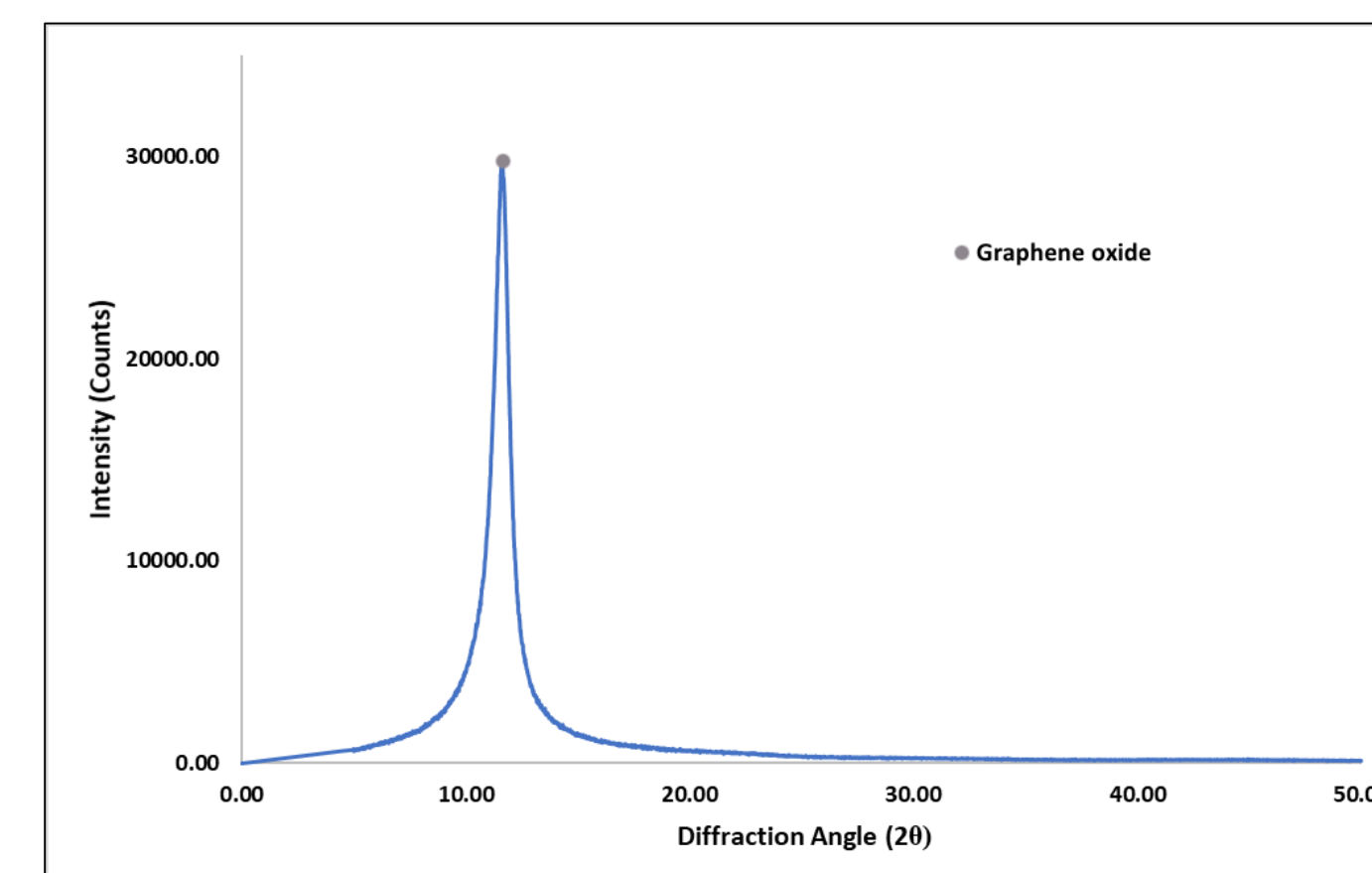


Figure 2: X-ray diffractogram of graphene oxide

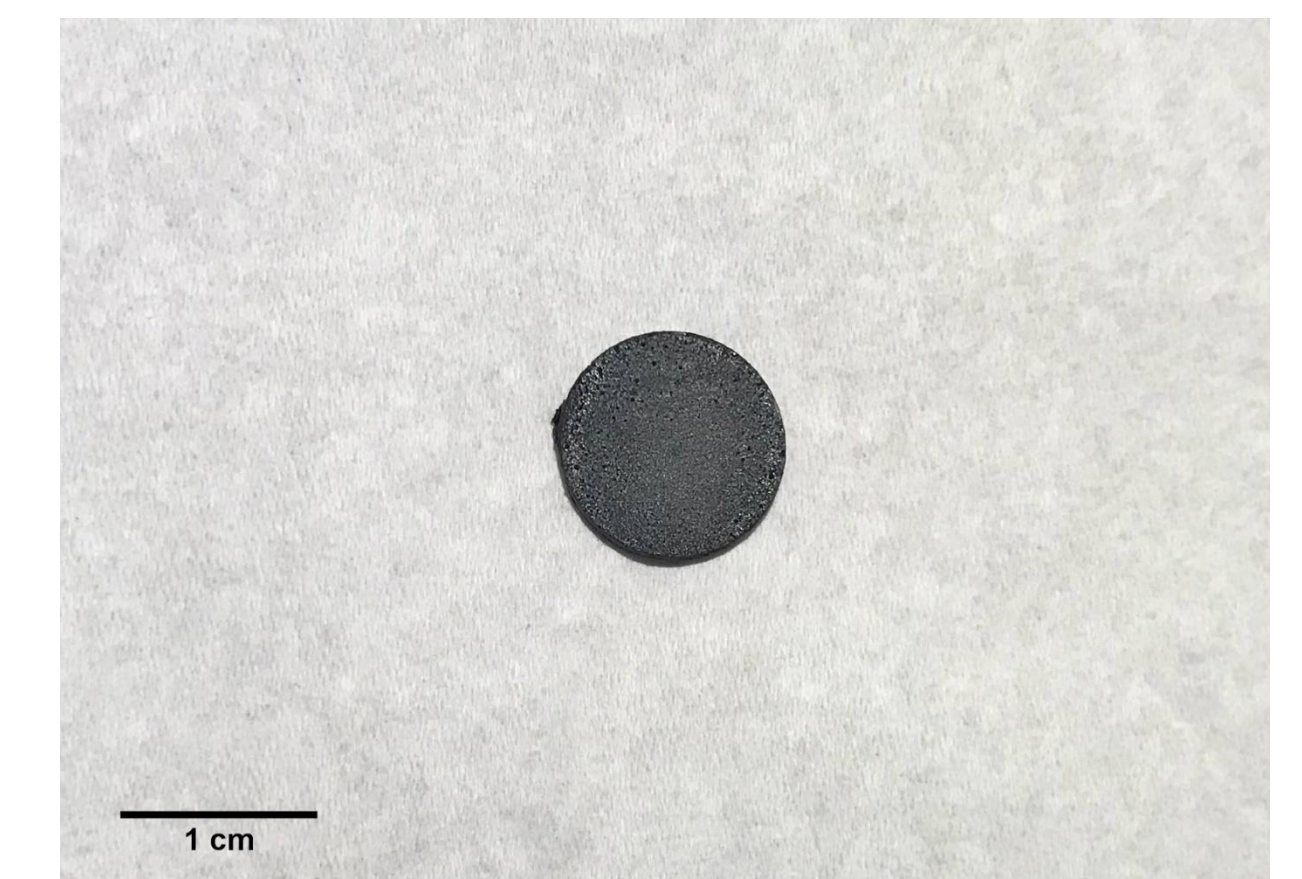


Figure 3: A UNS S41000 coupon coated with graphene oxide

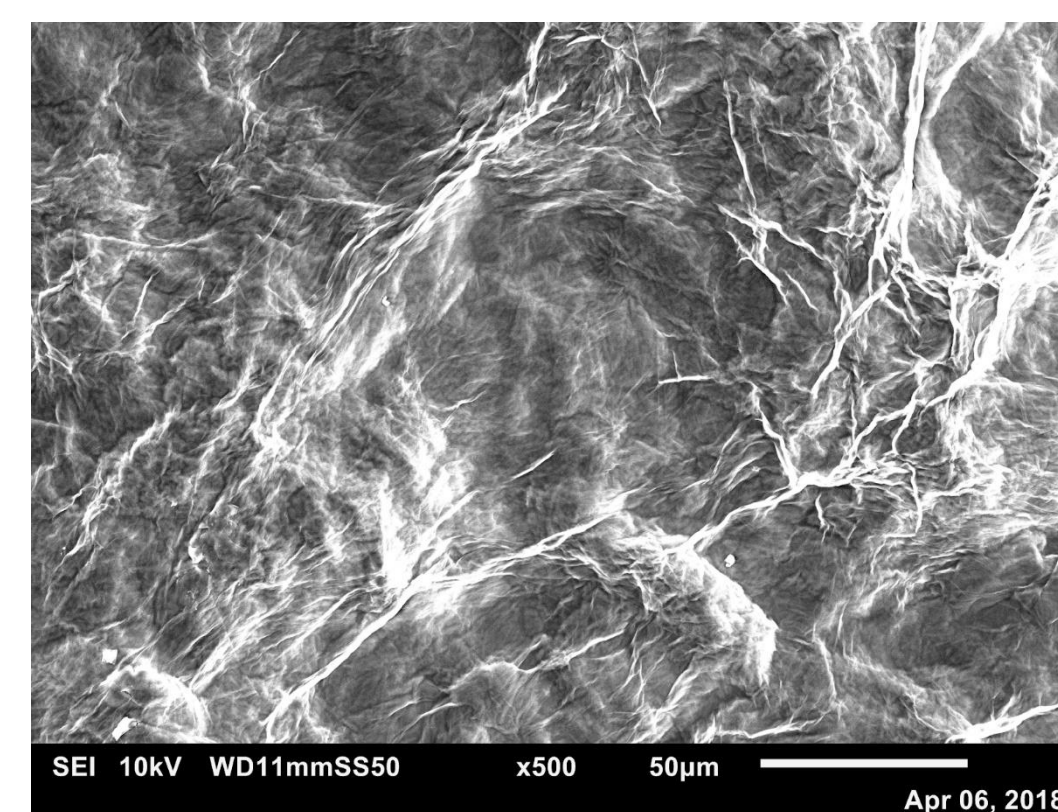


Figure 4: Secondary electron image of the graphene oxide precipitate

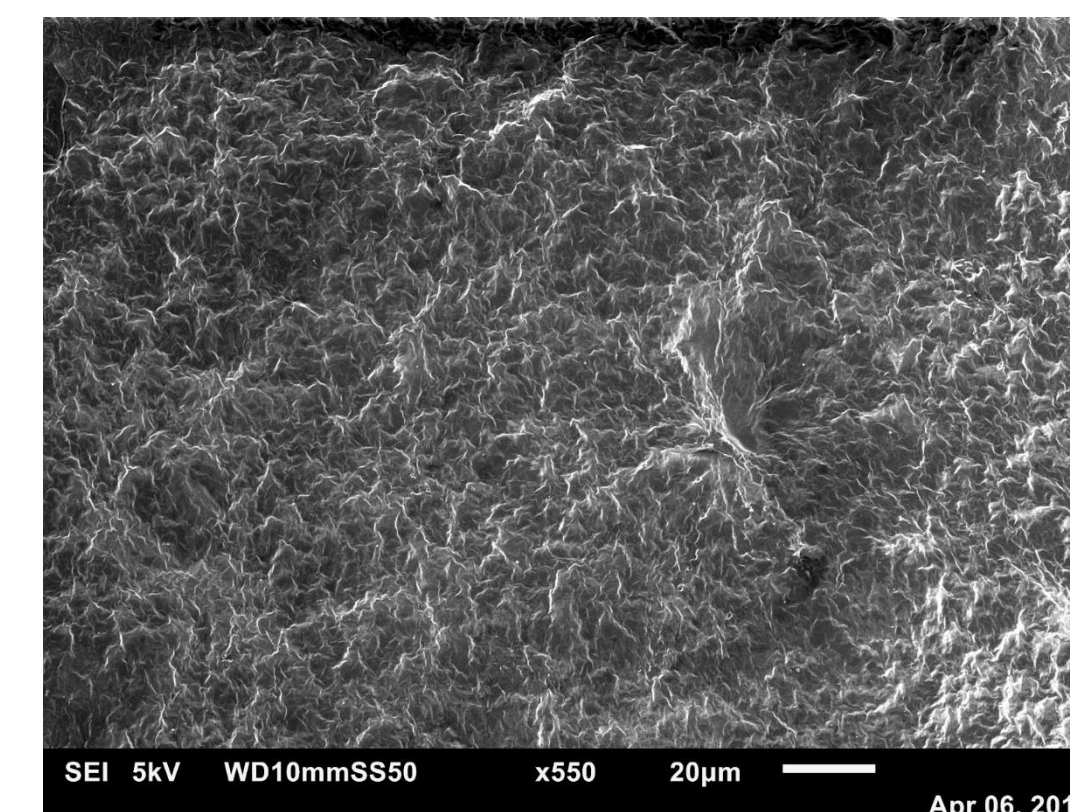


Figure 5: Secondary electron image of the surface of graphene oxide coated UNS S41000

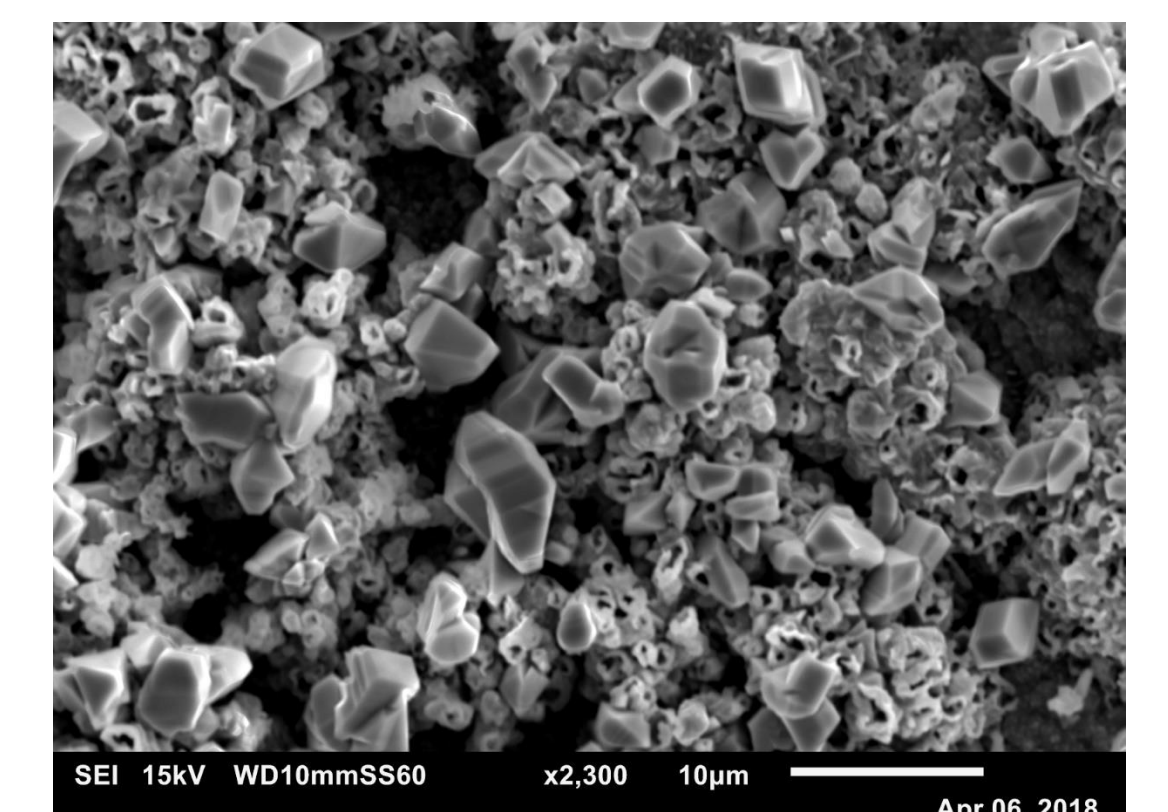


Figure 6: Secondary electron image of the surface of annealed graphene oxide coated UNS S41000

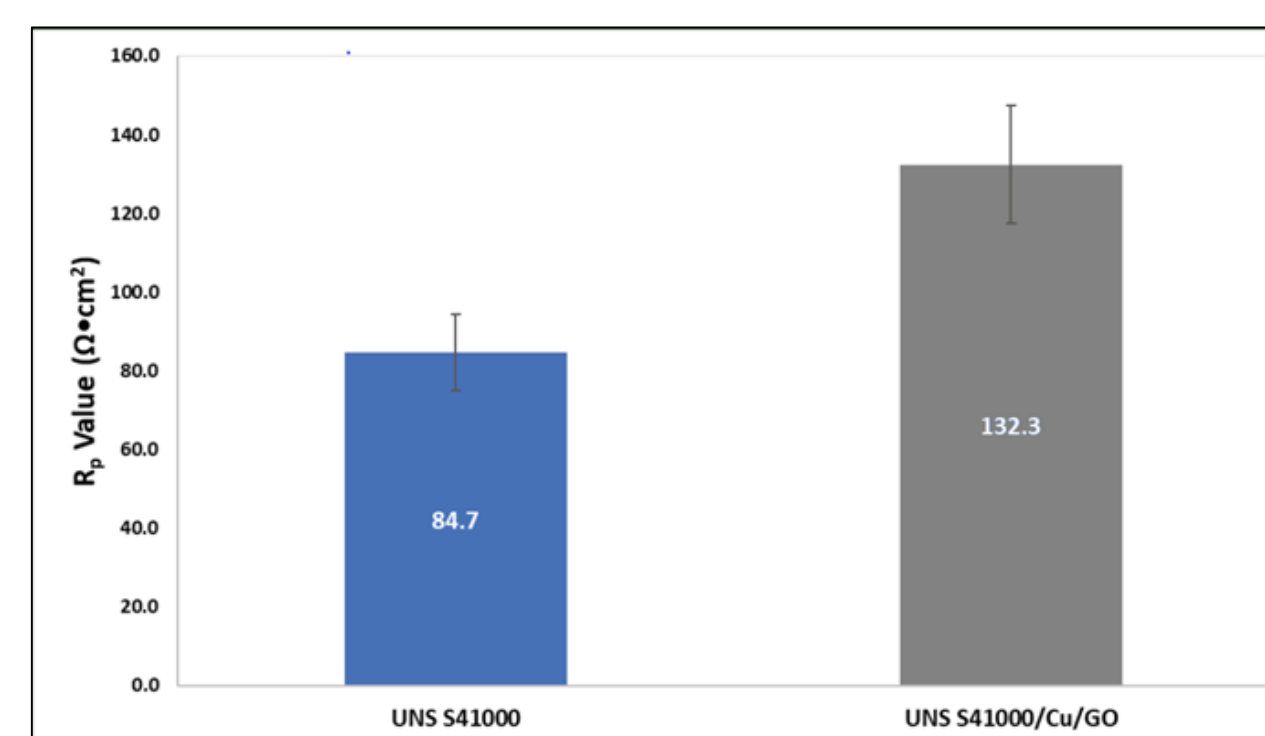


Figure 7: Resistance to polarization of uncoated and graphene oxide coated UNS

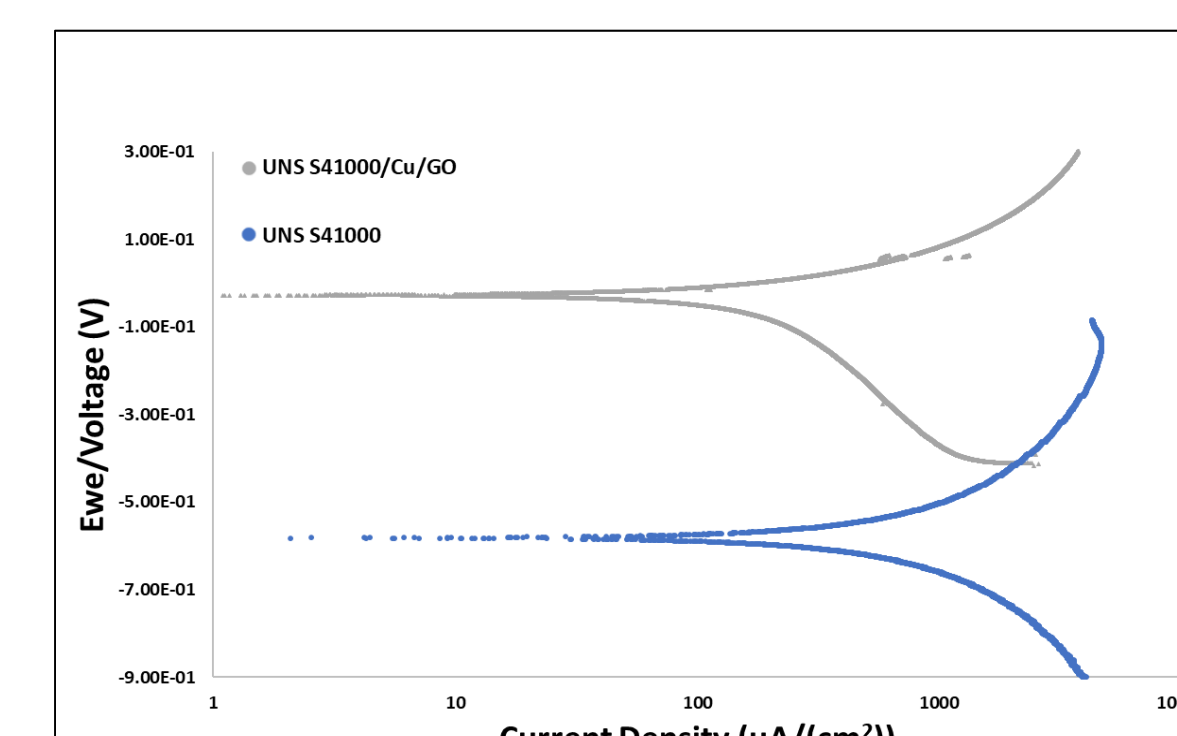


Figure 8: Tafel plots of uncoated and surface modified UNS S41000

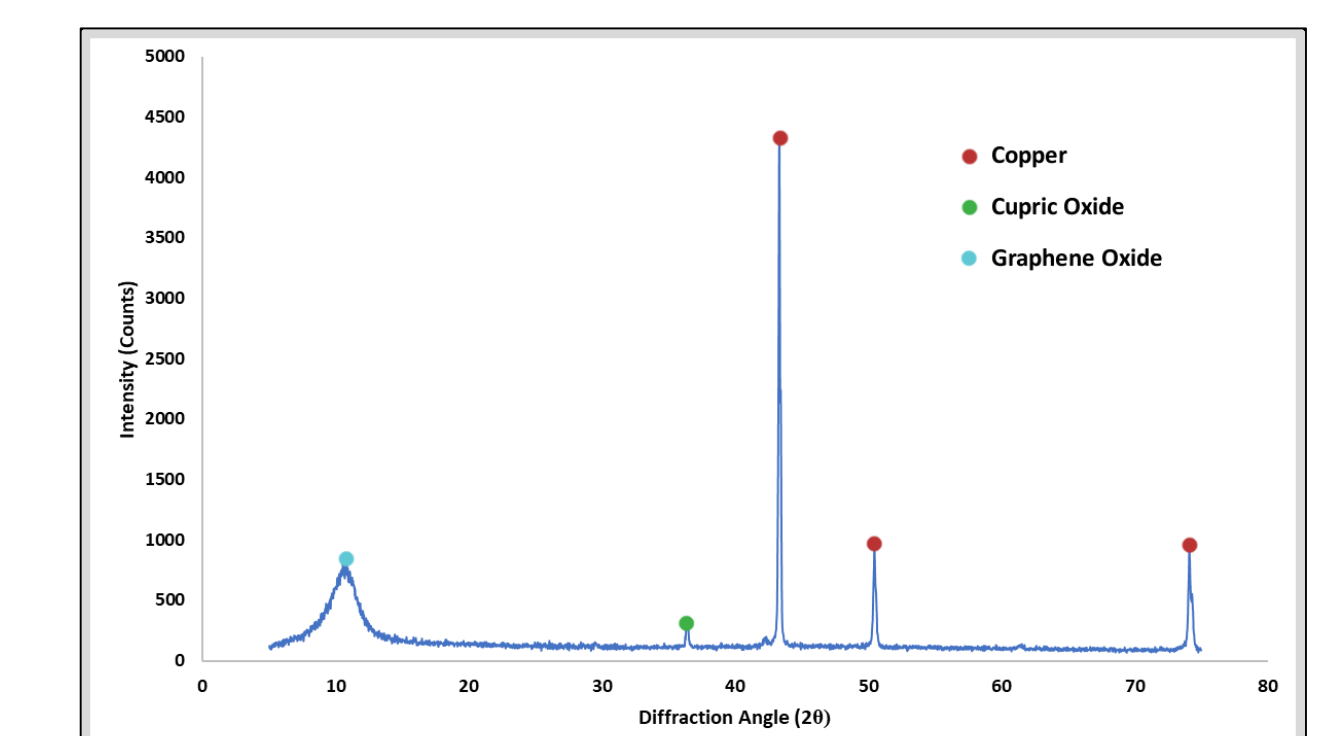


Figure 9: X-Ray diffractogram of copper and graphene oxide coated UNS S41000

Table 1: Average Values of i_{corr} and R_p values for uncoated and graphene oxide coated UNS S41000

Substrate	i_{corr} ($\mu\text{A}/\text{cm}^2$)	R_p (Ωcm^2)
UNS S41000	805.1 ± 259.2	84.7 ± 9.6
Coated UNS S41000	114.5 ± 50.4	132.2 ± 15.0
DOE 2020 Goals	<1	NA

Discussion:

Figure 1 shows the dried precipitate of graphene oxide obtained by the Tour Method. The X-Ray diffractogram, Figure 2, shows a strong peak at the diffraction angle, 2θ , of 10°, confirming that graphene oxide was successfully synthesized.⁵

Figure 3 shows graphene oxide coated UNS S41000. Figure 4 shows the secondary electron micrograph of the dried graphene precipitate. Figure 5 shows the surface topography of graphene oxide coated UNS 41000 coupon. The topographies obtained were consistent with previous literature.⁶ The topography of graphene oxide shown in Figure 6 corresponds to reduced graphene oxide⁷, as opposed to the partially reduced graphene oxide as seen in Figure 5. This hypothesis is further supported by Figure 9, where the XRD peaks show the presence of graphene oxide and copper, but no reduced graphene oxide peaks are observed. The graphene oxide coated coupon had a higher resistance to polarization compared to the uncoated coupon (Figure 7). The Tafel scan was performed on the uncoated and surface modified coupons (Figure 8). The calculated i_{corr} values were shown in Table 1, with uncoated UNS S41000 having a value of $805.1 \pm 259.2 \mu\text{A}/\text{cm}^2$ and the copper and graphene oxide coated UNS S41000 having a value of $114.5 \pm 50.4 \mu\text{A}/\text{cm}^2$. The coating reduces the i_{corr} by approximately a factor of 8; however, further i_{corr} reductions are anticipated using the fully reduced graphene oxide, i.e. graphene. More effective reduction methods are considered. Figure 6 shows an annealed sample where a reduced graphene oxide structure was achieved.

Summary and Conclusions:

The corrosion behavior of uncoated and surface modified UNS S41000 were characterized and compared in a simulated PEMFC environment using electrochemical techniques, SEM, and XRD.

Linear polarization resistance tests show that the surface modified UNS S41000 had a higher average resistance to polarization (R_p) value than the uncoated coupon. Additionally, the surface modified UNS S41000 had a significantly lower average i_{corr} value than the unmodified UNS S41000, indicating a higher corrosion resistance. More reductions in i_{corr} values are anticipated with a more complete reduction of graphene oxide to graphene. To achieve this outcome, alternative reduction methods, such as thermal reduction, are being explored.

Acknowledgements:

The authors would like to acknowledge Dr. Juan Nava, Anan S. Hamdan, Chris Faraj, Mauricio Paz, Joey Tulpinski, Ulus Ekerman (Cal Poly Pomona) and Jonathan Harris (Pomona College) for their support. The authors gratefully acknowledge financial support from Ms. Sylvia Hall, Drs. George and Mei Lai, the LA section of NACE International, Western States Corrosion Seminar, Western Area of NACE International, the NACE Foundation, the Boeing Company, California Steel Industries Inc. and the Southern California Chapter of the Association for Iron & Steel Technology. The SEM images and EDS analysis were made possible through a NSF MRI grant DMR- 1429674..